Metallurgy and materials
Metalurgia e materiais

Development of a new parameter for predicting hot metal desulfurization efficiency

Elton Volkers do Espírito Santo[1,2]
  https://orcid.org/0000-0002-2255-2274
Sábata Marla Reis Durães Oliveira[1,3]
  https://orcid.org/0000-0002-8492-8775
Caio Vaccari Silva[1,4]
  https://orcid.org/0000-0003-0851-6098
Felipe Fardin Grillo[1,5]
  https://orcid.org/0000-0002-0224-9075
José Roberto de Oliveira[1,6]
  https://orcid.org/0000-0003-3785-2306

[1]Instituto Federal de Educação, Ciência e Tecnologia do Espírito Santo - IFES, Departamento de Engenharia Metalúrgica e de Materiais, Vitória – Espírito Santo, Brasil.

E-mails: [2]elton.volkers@gmail.com,
[3]sabata.oliveira@gmail.com, [4]caio.vaccari@gmail.com,
[5]felipe.grillo@ifes.edu.br, [6]jroberto@ifes.edu.br

Abstract

Over the last decades, the capability of a desulfurizing mixture to remove sulfur has been widely studied. The hot metal desulfurization efficiency represents the percentage of sulfur removed from the bath and the development of parameters that predict the process efficiency is fundamental for selecting the best desulfurization mixture without the need for experimental tests. Therefore, this research aims to develop a new parameter to predict the hot metal desulfurization mixture efficiency, which was called the desulfurization factor (F_{DeS}). Desulfurizing mixtures from CaO-Fluorspar and CaO-Sodalite systems were used for this purpose. The phases present in the heating of the mixtures at 1400°C as well as the liquid and solid percentage were determined by ThelmoCalc software. These data were used in the desulfurization factor construction. Experiments were carried out in an electric resistance furnace with mechanical stirring. Different mixtures from these systems were added in molten hot metal at 1400°C. Sampling was made to measure the sulfur content variation with time. It was possible to apply the desulfurization factor to the proposed mixtures and to determine the influence of the solid and liquid phases on the desulfurization efficiency.

Keywords: hot metal; desulfurization; desulfurization factor; solid and liquid phases.

1. Introduction

Hot metal desulfurization in a Kambara Reactor is normally carried out with mixtures containing CaO and fluorspar (CaF_2). Its function is to decrease the solid phase amount that forms around the lime particle. However, fluorspar causes environmental problems and ladle refractory wear. Therefore, other fluxes are studied to replace fluorspar. Sodalite (Nepheline Syenite) is one of them. The hot metal desulfurization reaction can occur according to Equation 1 cited by Oeters (1985). Gibbs equation was obtained using data from Turkdogan and Martonik (1983).

$$[S] + CaO_{(s)} \rightarrow CaS_{(s)} + [O] \quad \Delta G^0 = 109{,}910 - 28.87T \text{ [J/mol]} \quad (1)$$

Depending on carbon and silicon content in hot metal, as well as SiO_2 and Al_2O_3 content in slag, there may also be the formation of carbon monoxide (CO), di or tricalcium silicate ($2CaO \cdot SiO_2$ and $3CaO \cdot SiO_2$), and tricalcium aluminate ($3CaO \cdot Al_2O_3$). The dicalcium silicate formation reaction occurs according to Equation 2, cited by McFeaters and Fruehan (1993). Gibbs equation was obtained using data from Turkdogan (1996).

$$4CaO_{(s)} + 2[S] + [Si] \rightarrow 2CaS_{(s)} + 2CaO \cdot SiO_{2(s)} \quad \Delta G^0 = -488{,}680 + 161.26T \text{ [J/mol]} \quad (2)$$

This reaction shows that the hot metal desulfurization process is exothermic since the first part of the Gibbs equation, that is, the enthalpy change, is negative. Therefore, if temperature increases, the equilibrium sulfur content also increases.

The desulfurization reaction generates solid phases like CaS, $3CaO \cdot SiO_2$, and $3CaO \cdot Al_2O_3$. These phases are formed around CaO particles. They reduce the interface area between CaO and the metal and hinder sulfur diffusion onto a CaO surface, decreasing the reaction rate and the desulfurization efficiency. This implies in steels with higher sulfur contents. Ohya *et al*. (1977) point out that when 15% of CaO particle is converted in CaS, the reagent desulfurizing power is practically annulled.

The effect of the solid phases on the desulfurization process can be decreased using a fluxing agent, since it dissolves the solid compounds into the liquid slag. Niedringhaus and Fruehan (1988), in their experiments, showed that liquid phase formation is critical for effective desulfurization. According to the authors, the solid phase amount decreases with the increase in liquid phase content. According to Chushao and Xin (1992), the rate constant increases for CaF_2 contents in the range of 0 – 10 wt.% for the CaO-CaF_2 mixtures. However, it does not occur for CaF_2 contents higher than 10 wt.%. Niedringhaus and Fruehan (1988) indicate that 5 wt.% of CaF_2 at 1450°C form 20 wt.% of liquid phase, which is sufficient to prevent solid phase formation.

To evaluate the sulfur removal thermodynamic efficiency by a desulfurizing mixture, normally these parameters are used: optical basicity (Λ), sulfide capacity (C_s), and sulfur partition coefficient (L_s). Sosinsky and Sommerville (1986) determined optical basicity values for some elements used in desulfurizing mixtures: CaO = 1; MgO = 0.78; CaF_2 = 0.37; SiO_2 = 0.48; Al_2O_3 = 0.61; P_2O_5 = 0.40; Na_2O = 1.15. Young (1991) defined sulfide capacity as the slag capacity to absorb sulfur. The author established relationships between sulfide capacity and optical basicity, which is shown by Equations 3 and 4.

$$log\,C_s = -13.913 + 42.84\Lambda - 23.82\Lambda^2 - \frac{11{,}710}{T} - 0.02223\%SiO_2 - 0.02275\%Al_2O_3 \qquad (3)$$

$$C_s = -0.6261 + 0.4808\Lambda - 0.7917\Lambda^2 + \frac{1{,}697}{T} - \frac{2{,}587\Lambda}{T} + 0.0005144\%FeO \qquad (4)$$

Equation 3 is valid for slags with $\Lambda < 0.8$ and Equation 4 is valid for slags with $\Lambda \geq 0.8$.

According to Turkdogan (1996), the sulfur partition coefficient (L_s) is a parameter that expresses the relationship between sulfur concentration in slag ($\%S_{eq.}$) and the metal bath [$\%S_{eq.}$] through the thermodynamic equilibrium. Inoue and Suito (1982) proposed an L_s model shown in Equation 5, which is a function of C_s, temperature, and hot metal dissolved elements.

$$log\,L_s = log\,C_s - \frac{1{,}053}{T} + 5.73 + log\,f_s \qquad (5)$$

Besides the mentioned models, there are others in literature, such as those proposed by Taniguchi, Sano, and Seetharaman (2009). These models were developed to evaluate the thermodynamic capacity of the mixture to remove sulfur from the bath. In addition, these models do not provide information about viscosity, liquid and solid amount, and phases present in the mixtures. Consequently, they do not provide the desulfurization kinetics. Aguiar *et al*. (2012) and Grillo (2015) related that these models can lead to erroneous conclusions concerning the selection of desulfurization mixtures, since they found no relationship between these models (Λ, C_s, and L_s) and desulfurization efficiency. The best thermodynamic results are not necessarily the best real results, which depend on kinetic factors, such as sulfur mass transfer.

The knowledge about the parameters that influence the desulfurization kinetics (phases present, liquid, and solid percentage and viscosity) is important since often the restriction for obtaining lower sulfur levels in industrial processes is not thermodynamic but kinetic.

The desulfurization rate is controlled by the sulfur diffusion until the CaO particle and it can be described by Equation 6 (Choi, Kim and Lee, 2001).

$$-\frac{d[\%S]}{dt} = k' \times \left(\frac{A}{V_m}\right) \times ([\%S]_t - [\%S]_{eq}) \qquad (6)$$

where A is the surface area between the CaO and the liquid metal (m²); k is the global coefficient of mass transportation (m/min); V is the hot metal volume; [$\%S$]$_t$ is the sulfur percentage at time t, and [$\%S$]$_{eq}$ is the equilibrium sulfur percentage.

Grillo *et al*. (2013) also state that computational thermodynamics is a tool that allows the determination of these parameters, and also the prediction of which mixture will be more efficient in industrial processes. In the last years, some researchers developed models for predicting desulfurization efficiency using these parameters in desulfurization and dephosphorization mixtures for hot metal and steel (Broseghini *et al*., 2018; Pezzin *et al*., 2020; Silva *et al*., 2020).

For the present research, the solid phases formed in the desulfurizing mixtures were taken into consideration for creating a new parameter to predict desulfurization efficiency. Based on thermodynamic simulation data, this parameter measures the amount of free lime available to react with sulfur, since the solid phases are formed on the lime surface and hence hinder the sulfur mass transport. Predicting the desulfurization performance of a desulfurizing mixture is fundamental for selecting the best mixture for industrial processes, since it spares time and raw materials which would be used for testing in the desulfurization facility.

Therefore, this research aims to develop a new parameter to predict the hot metal desulfurization mixture's efficiency,

which was called the desulfurization factor (F_{DeS}). Desulfurizing mixtures from CaO-Fluorspar and CaO-Sodalite systems were used. The phases present in the heating of the mixtures at 1400°C, as well as the liquid and solid percentage, were determined by ThelmoCalc software. These data were used in the desulfurization factor construction.

2. Materials and methods

2.1 Determination and characterization of the desulfurizing mixtures and hot metal

For the present study, the desulfurizing mixture's chemical composition was initially defined. It was obtained based on the raw material's chemical composition (lime, fluorspar, and nepheline). All these materials were provided by Tecnosulfur, including their particle size distribution. The lime had 89% of the particle size less than 38 μm, while fluorspar and nepheline had particle size less than 1.0 mm. Hot metal was also provided by Tecnosulfur. In each test, 1 kg of hot metal was used. The raw materials and hot metal chemical composition were determined by X-ray fluorescence (PANalytical - Axios Advanced) at IFES.

Table 1 shows the raw materials chemical composition.

Table 1 - Raw materials' chemical composition.

Material	Chemical composition (%)						
	CaO	CaF_2	Al_2O_3	SiO_2	Na_2O	C.L*	V.M**
Lime	90.0	-	0.3	2.0	-	7.7	-
Fluorspar	1.35	85.0	3.0	8.0	-	2.41	0.2
Nepheline	2.0	-	22.0	52.0	12.0	10.2	1.8

*C.L: Calcination Loss due to $CaCO_3$ e Na_2CO_3 decomposition; **Volatile Materials.

Table 2 shows the hot metal chemical composition.

Table 2 - Hot metal initial chemical composition.

Mixture	Initial Chemical Composition (%)				
	C	Mn	Si	P	S
F5	4.50	0.21	0.50	0.13	0.028
F5-S	4.48	0.21	0.50	0.13	0.028
F10	4.47	0.20	0.48	0.11	0.031
F10-S	4.49	0.19	0.48	0.11	0.031
N5	4.44	0.19	0.47	0.13	0.036
N10	4.52	0.19	0.51	0.12	0.028

The consumption of desulfurizing mixtures used on an industrial scale is normally 10 kg/ton of hot metal. For this reason, in this research, a ratio of 10 g/kg of hot metal was used in the experimental tests. Initially, the mixture's mass was 10 g. However, the contact between these mixtures and hot metal provokes loss by calcination and volatile materials. The mixtures proposed are summarized in Table 3.

Table 3 - Initial chemical composition and mixtures mass used in the experiments.

Mixtures	Chemical composition (%)					Mass(g)	Mass loss (g)
	CaO	Na_2O	CaF_2	Al_2O_3	SiO_2		
F5	92.50	-	4.70	0.42	2.49	9.26	0.74
F5-S	89.35	-	4.70	0.42	5.50	9.58	0.42
F10	87.43	-	9.16	0.61	2.80	9.28	0.72
F10-S	84.12	-	9.13	0.62	5.80	9.64	0.36
N5	92.95	0.65	-	1.50	4.90	9.21	0.79
N10	88.38	1.30	-	2.70	7.62	9.19	0.81

As can be seen in Table 3, mixtures with different contents of CaO, CaF_2, SiO_2, Al_2O_3, and Na_2O were used, with contents that are close to those used in industry. Mixtures F5 and F10 were made with 5 wt.% and 10 wt.% of fluorspar while mixtures F5-S and F10-S were made increasing SiO_2 content in 3 wt.% in mixtures F5 and F10. Mixtures N5 and N10 were made with 5 wt.% and 10 wt.% of nepheline.

2.2 Experimental procedure

Initially, solid hot metal was charged in MgO crucibles and then in an electrical resistance furnace MAI-TEC, model 1700-FEE/ at 1400°C. Further, argon gas (99.997% Ar) was injected onto the hot metal surface with a flow rate of 10Nl/min to prevent metal oxidation. After hot metal melting, a metal sample was removed, and then, the desulfurizing mixture was added to the metal bath through a stainless steel tube. After this step, samples were taken at 10, 15, 20, and 30 minutes. The samples were taken using glass vacuum samplers. Figure 1 shows a schematic diagram of the experimental setup used. Only one test was performed for each mixture.
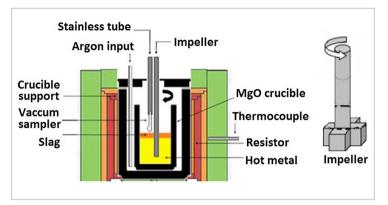

Figure 1 - Experimental setup schematic diagram.

The mechanical stirrer used is equipped with a 4-vane impeller to simulate desulfurization in a Kambara Reactor. The mechanical rotation was 400 rpm, since at this rotation the vortex formed in the bath showed a similar format compared to the vortex formed in industrial processes. Finally, the final sulfur concentration was determined through the samples taken by chemical analysis by direct infrared combustion in a LECO model CS-444 LS.

2.3 Determination of the phases present in the mixtures and sulfur equilibrium content

Through the desulfurizing mixtures and hot metal chemical compositions present in Tables 2 and 3, thermodynamic simulations were performed using the software ThermoCalc TCW v.5 and the database Slag3. The phases formed, the amount of solid and liquid phases in the mixtures, and the equilibrium sulfur concentration in the metal were identified at 1400°C.

2.4 Determination of the desulfurization factor (F_{DeS})

Equation 6 shows that the hot metal desulfurization reaction depends on the sulfur mass transport to the lime particle. In addition, the solid phases formed around the lime particles hinder the mass transport of sulfur. Based on Equation 6 and the phases obtained with ThermoCalc software, a new parameter could be determined. It was called the desulfurization factor (F_{DeS}) and was related to desulfurization efficiency. The expression of the F_{DeS} is shown in Equation 7.

$$F_{DeS} = (\%CaO_{(s)}) - (\%3CaO{\cdot}SiO_{2(s)} + \%3CaO{\cdot}Al_2O_{3(s)}) \quad (7)$$

where $\%CaO_{(s)}$: solid CaO and $\%3CaO{\cdot}SiO_{2(s)} + \%3CaO{\cdot}Al_2O_{3(s)}$: solid phases sum.

3. Results and discussion

Figure 2 shows sulfur variation with time and the desulfurization efficiency for each mixture.
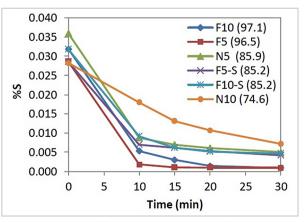

Figure 2 - Sulfur content variation with time.

The desulfurization efficiency (%η) was calculated by Equation 8:

$$\eta(\%) = \frac{[\%S_i] - [\%S_f]}{[\%S_i]} \times 100 \qquad (8)$$

Figure 2 indicates that the desulfurization rate is higher and constant until the first 10 minutes and most of the desulfurization (30 to 90%) occurs during this period. From 15 minutes on desulfurization rate decreases.

It is noted that the desulfurization rates are very similar among the mixtures for the first 10 minutes (except for mixture N10). The initial sulfur content varies from 0.02824 to 0.03600 and seems not to have a noticeable influence on the rate. Table 4 shows the equilibrium sulfur contents for each mixture and it is noted that those values have no direct relationship with the initial sulfur content. Besides, those values are nearly the same and are quite low and hence, do not influence the desulfurization rates. By analyzing Equation 6, it is noted that when the sulfur equilibrium content is low, it does not influence the reaction rate for the initial stages. In addition, it is expected that the higher the initial sulfur content, the faster the rate. However, this was not observed, prob-

ably due to the small difference between these values (only 77.6 ppm). Mixtures F5, F5-S and N10 contained 0.028% of sulfur and reached rates of 0.002672, 0.002160, and 0.001025 %S/min. Mixtures F10 and F10-S contained 0.031% of sulfur and reached rates of 0.002649, and 0.002260 %S/min. Mixture N5 contained 0.036% of sulfur and reached a rate of 0.002721 %S/min. It is observed that the rates are nearly the same in the first 10 minutes and mixture N10 showed a low desulfurization rate probably due to the formation of solid phases around lime particles (Table 4 shows that mixture N10 formed 30.2% of $3CaO \cdot SiO_2$ and $3CaO \cdot Al_2O_3$), which decreases both the surface area between CaO and the liquid metal (A) and the global coefficient of mass transportation (k') from Equation 6.

From 10 minutes ahead the rates decrease substantially owing to the decrease in sulfur content and hence the decrease in its availability (Equation 6 shows that the decrease in sulfur

content at time t decreases the driving force of the desulfurization reaction and hence decreases the rate). At the same time, the formation of solid phases in the mixtures also hampers sulfur diffusion. At this point, the rate of mixture N10 is the highest due to the higher sulfur content compared with the other mixtures.

It is possible to note in Figure 2 that F5 and F10 mixtures reached higher desulfurization efficiency, with 96.5% and 97.1%, respectively. Doubling fluorspar addition in mixture F10 increased efficiency by 0.6%, which indicates that 5 wt.% of fluorspar is enough for reaching low sulfur contents. N5 and N10 mixtures showed lower efficiency than those obtained by F5 and F10 mixtures, with 85.9% and 74.6%, respectively.

Table 4 shows the initial, final, and equilibrium sulfur content, the phases formed, and solid and liquid percentages in the mixtures at 1400°C obtained by software ThermoCalc.

Table 4 - Sulfur contents (%S_{eq}, %S_i and %S_f) and phases formed in the tests.

Mixture	%Liquid	Solid phases formed (%)				%S_{eq}	%S_i	%S_f	η(%)
		$CaO_{(s)}$	C_3S	C_3A	$C_3S + C_3A$				
F10	18.7	81.3	-	-	-	$1.54 \cdot 10^{-5}$	0.03185	0.00093	97.1
F5	9.2	85.1	5.7	-	5.7	$1.57 \cdot 10^{-5}$	0.02858	0.00099	96.5
N5	2.4	77.9	16.2	3.5	19.7	$1.53 \cdot 10^{-5}$	0.03600	0.00506	85.9
F5-S	8.8	74.5	16.6	-	16.6	$1.61 \cdot 10^{-5}$	0.02860	0.00423	85.2
F10-S	16.8	69.0	14.2	-	14.2	$1.55 \cdot 10^{-5}$	0.03180	0.00471	85.2
N10	4.8	65.0	24.1	6.1	30.2	$1.56 \cdot 10^{-5}$	0.02824	0.00718	74.6

CaOS: Solid CaO percentage that was not used to form C_3S and/or C_3A; C_3S: $3CaO \cdot SiO_2$; C_3A: $3CaO \cdot Al_2O_3$.

Table 4 also shows the liquid and solid amounts and the phases formed in the mixtures. It can be noticed that mixtures F10 and F5 show a higher liquid amount than mixtures N5 and N10.

Taking the equilibrium sulfur contents into account, it can be said that the mixtures have the same thermodynamic capacity to remove sulfur. Therefore, the differences in the desulfurization efficiency are due to kinetic

parameters, which in the present study are the solid phases that form around the lime particle. This cover hinders the sulfur mass transfer from the bath to the CaO particle. In addition, none of the mixtures achieved the equilibrium sulfur content.

Table 4 shows that mixtures containing higher SiO_2 and Al_2O_3 content form more compounds which may limit sulfur mass transfer: tricalcium

silicate ($3CaO \cdot SiO_2$) and tricalcium aluminate ($3CaO \cdot Al_2O_3$), as discussed by Niedringhaus and Fruehan (1988).

Table 4 shows that all mixtures showed a reduction in total solid CaO concentration. This occurred because a part of CaO formed the solid phases $3CaO \cdot SiO_2$ and/or $3CaO \cdot Al_2O_3$ and another part formed the liquid phase, as shown in Table 5, which shows the liquid phase chemical composition.

Table 5 - Liquid phase chemical composition.

Mixtures	%CaO	%Na$_2$O	%CaF$_2$	%Al$_2$O$_3$	%SiO$_2$
F10	33.5	-	51.9	3.5	11.1
F5	34.9	-	49.4	5.1	10.6
N5	37.8	27.3	-	8.1	26.8
F5-S	34.7	-	48.9	5.9	10.5
F10-S	33.6	-	51.8	3.5	11.1
N10	37.8	27.3	-	8.1	26.8

Therefore, by heating the desulfurizing mixtures at 1400°C, it is expected that mixtures F5 and F10 show better results than mixtures N5 and N10. Table 4 also shows that the mixtures with higher efficiency, F5 and F10, had higher liquid slag amount, lower tricalcium silicate (3CaO·SiO$_2$) formation, and higher solid CaO amount (CaO percentage that was not used to form 3CaO·SiO$_2$ and/or 3CaO·Al$_2$O$_3$).

Figure 3 shows the relationship between liquid phase, total solid CaO, and solid phase's concentration with the desulfurization efficiency.
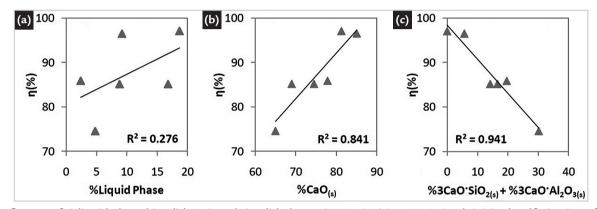

Figure 3 - Influence of a) liquid phase b) solid CaO and c) solid phases (%3CaO·SiO$_2$ + %3CaO·Al$_2$O$_3$) in desulfurization efficiency.

Figure 3a shows that the coefficient of determination between the liquid phase amount and the efficiency was low (R^2 = 0.276). This is an indication that the liquid phase formed has no direct influence on the desulfurization reaction, acting only in the solid phase dissolution. Figure 3b shows that the increase in solid CaO amount is related to the increase in the desulfurization efficiency, that is, the higher the CaO available to react, the lower the hot metal sulfur content. Figure 3c shows that the coefficient of determination between solid phases (3CaO·SiO$_2$ and 3CaO·Al$_2$O$_3$) and efficiency was 0.941, which was the highest one. This indicates that the formation of 3CaO·SiO$_2$ and 3CaO·Al$_2$O$_3$ around lime particles causes a decrease in desulfurization efficiency.

As desulfurization occurs by the direct reaction between CaO particles and sulfur in hot metal, it should be considered that CaO particles are effectively available to react. Then, to analyze the influence of these parameters in desulfurization efficiency, another parameter was created: the desulfurization factor (F_{DeS}), which is shown in Equation 9.

$$F_{DeS} = (\%CaO_{(s)}) - (\%3CaO·SiO_{2(s)} + \%3CaO·Al_2O_{3(s)}) \quad (9)$$

where %CaO$_{(s)}$: solid CaO and %3CaO·SiO$_{2(s)}$ + %3CaO·Al$_2$O$_{3(s)}$: solid phases sum.

Therefore, the desulfurization factor represents the amount of CaO that is effectively available to react with the sulfur present in the metal bath. Figure 4 shows its influence on desulfurization efficiency.
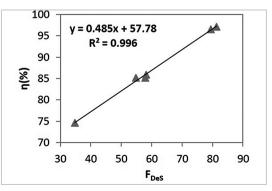

Figure 4 - F_{DeS} influence on desulfurization efficiency.

According to Figure 4, the mixtures with higher efficiency were the same with higher F_{DeS} value, since high F_{DeS} indicates less solid phases formed around CaO particles. This leads to a higher global mass transfer coefficient shown in Equation 6, which increases desulfurization efficiency. Then, from the linear regression equation, present in the Figure 4 graph, it is possible to develop a relationship to predict the efficiency of the mixtures. This is shown in Equation 10 and Equation 11.

$$\eta(\%) = 0.485 \times (F_{DeS}) + 57.78 \tag{10}$$

$$\eta(\%) = 0.485 \times [(\%CaO_{(s)}) - (\%3CaO \cdot SiO_{2(s)} + \%3CaO \cdot Al_2O_{3(s)})] + 57.78 \tag{11}$$

The coefficient of determination for the linear regression between the desulfurization factor and efficiency was 0.996, almost 1. This led to the conclusion that the solid compounds $3CaO \cdot SiO_2$ and $3CaO \cdot Al_2O_3$ limits the CaO desulfurizing power due to their formation around the lime surface, which decreases the global mass transfer coefficient and hence, the efficiency.

It is important to mention that this expression is applied only to mixtures with the same characteristics as those used in this research and under the same experimental conditions.

Based on these results, it can be stated that ThermoCalc provides information and data which help to predict the desulfurization mixture's efficiency. Thus, it is also possible to state that the best hot metal desulfurizing mixture is the one that shows the following properties when added to the bath: higher liquid phase percentage and, consequently, a lower solid phase percentage; less tricalcium silicate ($3CaO \cdot SiO_2$) formation; less tricalcium aluminate ($3CaO \cdot Al_2O_3$) formation and higher solid CaO concentration in the slag.

4. Conclusions

The desulfurization factor proved to be a useful parameter to predict the efficiency of mixtures from CaO-Fluorspar and CaO-Sodalite systems since the coefficient of determination was 0.996. Increasing the desulfurization factor also increases efficiency. This result reinforces that the knowledge regarding the phases present and the liquid and solid percentage is important for understanding the process and for selecting the best desulfurizing mixture.

In addition, efficiency was lower for mixtures that formed lower solid CaO and higher $3CaO \cdot SiO_2$ and $3CaO \cdot Al_2O_3$ amounts. The liquid phase acts on the solid phase dissolution and has no direct relation to desulfurization efficiency for this type of mixture.

Acknowledgments

References

AGUIAR, F. N.; OLIVEIRA, H. C. C.; DAVID, S. F.; NASCIMENTO, R. C.; OLIVEIRA, J. R. Parâmetros termodinâmicos e cinéticos de misturas dessulfurantes à base de CaO, MgO, SiO_2 e CaF_2. *Tecnologia em Metalurgia, Materiais e Mineração*, v. 9, n. 3, p. 242-249, 2012.

BROSEGHINI, F. C.; OLIVEIRA, H. C. C.; SOARES, S. G.; GRILLO, F. F.; OLIVEIRA, J. R. Evaluating the hot metal dephosphorization efficiency of different synthetic slags using phosphorus partition ratio, phosphate capacity and computational thermodynamics. *REM - International Engineering Journal*, v. 71, n. 2, p. 217-223, 2018.

CHOI, J. Y.; KIM, D. J.; LEE, H. G. Reaction kinetics of desulfurization of molten pig iron using $CaO–SiO_2–Al_2O_3–Na_2O$ slag systems. *ISIJ International*, v. 41, n. 3, p. 216-224, 2001.

CHUSHAO, X.; XIN, T. The kinetics of desulfurization of hot metal by $CaO-CaF_2$ based fluxes. *ISIJ International*, v. 32, n. 10, p. 1081-1083, 1992.

GRILLO, F. F. *Estudo da substituição da fluorita por alumina ou sodalita e de cal por resíduo de mármore em escórias sintéticas dessulfurantes*. 2015. 172 f. Tese (Doutorado em Engenharia Metalúrgica e de Materiais) – Escola Politécnica, Universidade de São Paulo, São Paulo, 2015.

INOUE, R.; SUITO, H. Sulfur partitions between carbon-saturated iron melt and Na_2O-SiO_2 slags. *Transactions ISIJ*, v. 22, n. 7, p. 514-523, 1982.

MCFEATERS, L. B.; FRUEHAN, R. J. Desulfurization of bath smelter metal. *Metallurgical Transactions B*, v. 24, n. 3, p. 441-447, 1993.

NIEDRINGHAUS, J. C.; FRUEHAN, R. J. Reaction mechanism for the CaO-Al and $CaO-CaF_2$ desulfurization of carbon-saturated iron. *Metallurgical Transactions B*, v. 19B, n. 2, p. 261-268, 1988.

OETERS, F. Kinetic treatment of chemical reactions in emulsion metallurgy. *Steel Research*, v. 56, n. 2, p. 69-74, 1985.

OHYA, T.; KODAMA, F.; MATSUNAGA, H.; MOTOYOSHI, M.; HIGASHIGUCHI, M. Desulfurization of hot metal with burnt lime. *In*: NATIONAL OPEN HEARTH AND BASIC OXYGEN STEEL CONFERENCE, 60., 1977, Pittsburgh. *Proceedings* […]. Englewood, Colorado: AIME, 1977. p. 345-355.

PEZZIN, R. O.; BERGER, A. P. L.; GRILLO, F. F.; JUNCA, E.; FURTADO, H. S.; OLIVEIRA, J. R. Analysis of the influence of the solid and liquid phases on steel desulfurization with slags from the $CaO-Al_2O_3$ systems using computational thermodynamics. *Journal of Materials Research and Technology*, v. 9, n. 1, p. 838-846, 2020.

SILVA, C. V.; BROSEGHINI, F. C.; JUNCA, E.; GRILLO, F. F.; OLIVEIRA, J. R. Use of computational thermodynamics software to determine the influence of CaO, FeO and SiO$_2$ on hot metal dephosphorization efficiency. *Journal of Materials Research and Technology*, v. 9, n. 5, p. 10529-10536, 2020.

SOSINSKY, D. J.; SOMMERVILLE, I. D. The composition and temperature dependence of the sulfide capacity of metallurgical slags. *Metallurgical Transactions B*, v. 17B, n. 2, p. 331-337, 1986.

TANIGUCHI, Y.; SANO, N.; SEETHARAMAN, S. Sulphide capacities of CaO-Al$_2$O$_3$-SiO$_2$-MgO-MnO slags in the temperature range 1673-1773 K. *ISIJ International*, v. 49, n. 2, p. 156-163, 2009.

TURKDOGAN, E. T. Fundamentals of steelmaking. London: The Institute of Materials, 1996. 331 p.

TURKDOGAN, E. T.; MARTONIK, L. J. Sulfur solubility in iron-carbon melts coexistent with solid CaO and CaS. *Transactions ISIJ*, v. 23, n. 12, p. 1038-1044, 1983.

YOUNG, R. W. Calculations using the data bank. In: YOUNG, R. W. *Use of the optical basicity concept for determining phosphorus and sulphur slag/metal partitions.* London: British Steel, 1991. p. 5-8.

.